

# Characteristics of Fluid Flow and Heat Transfer in a Fluidized Heat Exchanger with Circulating Solid Particles

Soo Whan Ahn\*, Byung-Chang Lee\*\*, Won-Cheol Kim, Myung-Whan Bae

School of Transport Vehicle Engineering, Institute of Marine Industry,  
Gyeongsang National University, Kyongnam 650-160, Korea

Yoon Pyo Lee

Thermal/Flow Control Research Center, Korea Institute of Science of Technology,  
Seoul 136-791, Korea

The commercial viability of heat exchanger is mainly dependent on its long-term fouling characteristic because the fouling increases the pressure loss and degrades the thermal performance of a heat exchanger. An experimental study was performed to investigate the characteristics of fluid flow and heat transfer in a fluidized bed heat exchanger with circulating various solid particles. The present work showed that the higher densities of particles had higher drag force coefficients, and the increases in heat transfer were in the order of sand, copper, steel, aluminum, and glass below Reynolds number of 5,000.

**Key Words :** Fluidized Bed Heat Exchanger, Solid Particle, Heat Transfer Coefficient, Drag Coefficient, Fouling

## Nomenclature

$A$  : Contact surface [ $m^2$ ]  
 $C_d$  : Drag coefficient  
 $d$  : Diameter [ $m$ ]  
 $F_b$  : Buoyancy force [ $N$ ]  
 $F_d$  : Resistance force [ $N$ ]  
 $F_g$  : Gravity force [ $N$ ]  
 $g$  : Gravity acceleration [ $m/s^2$ ]  
 $h$  : Heat transfer coefficient [ $W/m^2K$ ]  
 $m$  : Mass [ $kg$ ]  
 $\dot{m}$  : Flow rate [ $kg/s$ ]  
 $Nu$  : Nusselt number  
 $Re$  : Reynolds number  
 $U_r$  : Relative velocity [ $m/s$ ]  
 $V$  : Water velocity in the tube [ $m/s$ ]

$\nu$  : Kinematic viscosity [ $m^2/s$ ]

## Subscripts

0 : Without solid particle  
 1 : Solid particle diameter  
 2 : Tube diameter  
 $b$  : Bulk  
 $p$  : Solid particle  
 $t$  : Tube  
 $w$  : Wall, water (fluid)

## 1. Introduction

Fouling is defined as deposition of unwanted materials on the heat transfer surfaces, which increases the pressure loss and degrades the thermal performance of a heat exchanger. Especially when the processing fluid contains foreign materials, fouling control becomes an important issue. In certain cases, the thermal fouling resistance exceeds half of the total thermal resistance. To remove the deposit, a number of techniques have been developed. They include both mechanical and chemical methods. In mechanical methods,

\* Corresponding Author,

E-mail : swahn@gachuk.gsnu.ac.kr

TEL : +82-55-640-3125; FAX : +82-55-640-3128

School of Transport Vehicle Engineering, Institute of Marine Industry, Gyeongsang National University, Tongyeong 650-160, Korea. (Manuscript Received November 24, 2001; Revised May 27, 2002)

\*\* (Present) Graduate School, Mechanical Engineering Department Changwon National University, Changwon, Kyongnam 641-060, Korea.

sponge balls or brushes are circulated with fluid, and remove the deposit. In chemical methods, which are more popular, chemicals such as chlorine or acid are added into the fluid to soften the deposit, and the flow eventually removes the deposit. However, added chemicals may induce secondary environmental problems, and additional pumps or valves are necessary to adopt the mechanical methods.

The different concepts to mitigate fouling of heat exchangers have been developed by highly specialized equipment such as fluidized bed heat exchangers. For proper design of circulating fluidized bed heat exchangers, it is important to know the effect of design and operating parameters on the bed to wall heat transfer coefficients and fluid flow characteristics. At present, there is a dearth of mechanistic models for predicting this effect. Grace (1986) inferred that the bed density had a major influence on heat transfer. This inference was based on experimental data of Fraley et al. (1983), Kiang et al. (1976), Stromberg (1982), and Mickley and Trilling (1949). The experimental investigation by Adomeit and Renz (1994) showed that the increase of flow rate led to a decrease of the effective particle transport rate to the exchanger surface. This is a contradiction to the general assumption that the increase of flow rate enhances transport as deduced from an analogy consideration. Lee et al. (2000) performed an experiment to measure heat transfer rates and pressure drops in a fluidized heat exchanger with circulating solid particles in air at a constant heat transfer rate. Lee et al. (1995) studied the characteristics of self-cleaning and heat transfer enhancement of a fluidized bed heat exchanger with circulating glass beads. The movement of spherical particles in a tube was visualized and heat transfer enhancement and scale reduction mechanism by particles was investigated. Kim and Lee (1995) measured the pressure loss and the heat transfer coefficient in a vertical tube with circulating three different diameter glass beads. They showed that, at low flow velocities, glass beads enhanced the heat transfer considerably. The enhancement increased with the volume fraction of the glass beads. The pres-

sure loss also showed a similar trend.

In present work, an experimental study has been conducted to check out the characteristics of fluid flow and heat transfer in a fluidized bed heat exchanger with circulating 7 different solid particles in water, such as glass (bead, 3 mm  $\Phi$ ), aluminum (cylinder, 2 mm  $\Phi$ , 4.5 mm L), aluminum (cylinder, 3 mm  $\Phi$ , 2 mm L), steel (cylinder, 2.0 mm  $\Phi$ , 4.5 mm L), steel (cylinder, 2.5 mm  $\Phi$ , 2.88 mm L), copper (cylinder, 2.5 mm  $\Phi$ , 2.88 mm L), and sand (grain, 2~4 mm  $\Phi$ ). Drag coefficients and heat transfer coefficients were measured. Fouling tests were also performed with ferric oxide as a foulant.

## 2. Experimental Apparatus and Test Procedure

The combined experimental apparatus was built to measure the pressure drop, heat transfer, and to perform a flow visualization test as shown in Fig. 1. The apparatus consisted of a pump, valves, a water tank, two heat exchangers, a condensing coil, and a test section. The dimensions of the heat exchanger were 705 mm in height, 80.4 mm in shell diameter. The tubes for heat transfer and visualization had same inner diameters of 16.2 mm. Magnetic pump (190 W, PM-100 PD) was chosen because the wide impeller spacing made solid particles or foreign materials pass through easily. Flow rate was controlled by the valves which bypassed a relevant amount of water back to a reservoir, and the fluid flow rate in the tube was measured with a cumulative type flow meter and a timer, at which the minimum range was 10 ml. Downstream of the test section, a condensing coil was installed to maintain the constant temperature of circulating fluid at the entrance of test section. The test section and the fluidized bed heat exchanger (right hand side in Fig. 1) were fabricated with a transparent acrylic material for easy accessibility of CCD camera. Particle flow was visualized by a CCD camera. Particle velocity was determined from the moving distance and elapsed time. The heat transfer test section (left hand side in Fig. 1) was made of stainless steel (SUS 304). Both the fluidized bed

heat exchanger for heat transfer (left hand side) and that for visualization (right hand side) had same dimensions. Table 1 shows seven different particles used in experiment such as glass (bead, 3 mm dia.), aluminum (cylinder, 2 mm and 3 mm dia.), copper (cylinder, 2.5 mm dia.), steel (cylinder, 2 mm and 2.5 mm), and sand (grain, 2~4 mm dia.). All the particles had the same volume of 14 mm<sup>3</sup> except the sand. The U-type tube at inlet (see Fig. A1 in Appendix 1) and the screen

at exit prevented the particles from escaping out of the test section. The calculation procedure of water flow velocity (*V*) in a tube of heat exchanger and the principle of solid particle circulation are illustrated in Appendix 1. The force acting on the solid particle in the stream is shown in Fig. 2. Assuming the particle mass becomes *m<sub>p</sub>*, the gravity force (*F<sub>g</sub>*) is given by;

$$F_g = m_p g \tag{1}$$

The buoyancy force is attributed to density difference between the particle and the surrounding fluid, the buoyancy force (*F<sub>b</sub>*) is obtained from the fluid mass (*m<sub>w</sub>*) as follows;

$$F_b = m_w g \tag{2}$$

The drag force (*F<sub>d</sub>*) means the resultant force in terms of viscosity acted by a particle and the surrounding fluid. From an usual definition of friction factor, the drag force becomes;

$$F_d = 0.5 \rho_w U_r^2 C_d A \tag{3}$$

**Table 1** Details of particles in fluidized bed

Classification	Material	Geometry	Dimension
Case (A)	glass	bead	3 mm $\Phi$
Case (B)	Al	cylinder	2 mm $\Phi$ , 4.5 mmL
Case (C)	Al	cylinder	3 mm $\Phi$ , 2 mmL
Case (D)	steel	cylinder	2 mm $\Phi$ , 4.5 mmL
Case (E)	steel	cylinder	2.5 mm $\Phi$ , 2.88 mmL
Case (F)	Cu	cylinder	2.5 mm $\Phi$ , 2.88 mmL
Case (G)	sand	grain	2.0 mm~4.0 mm $\Phi$

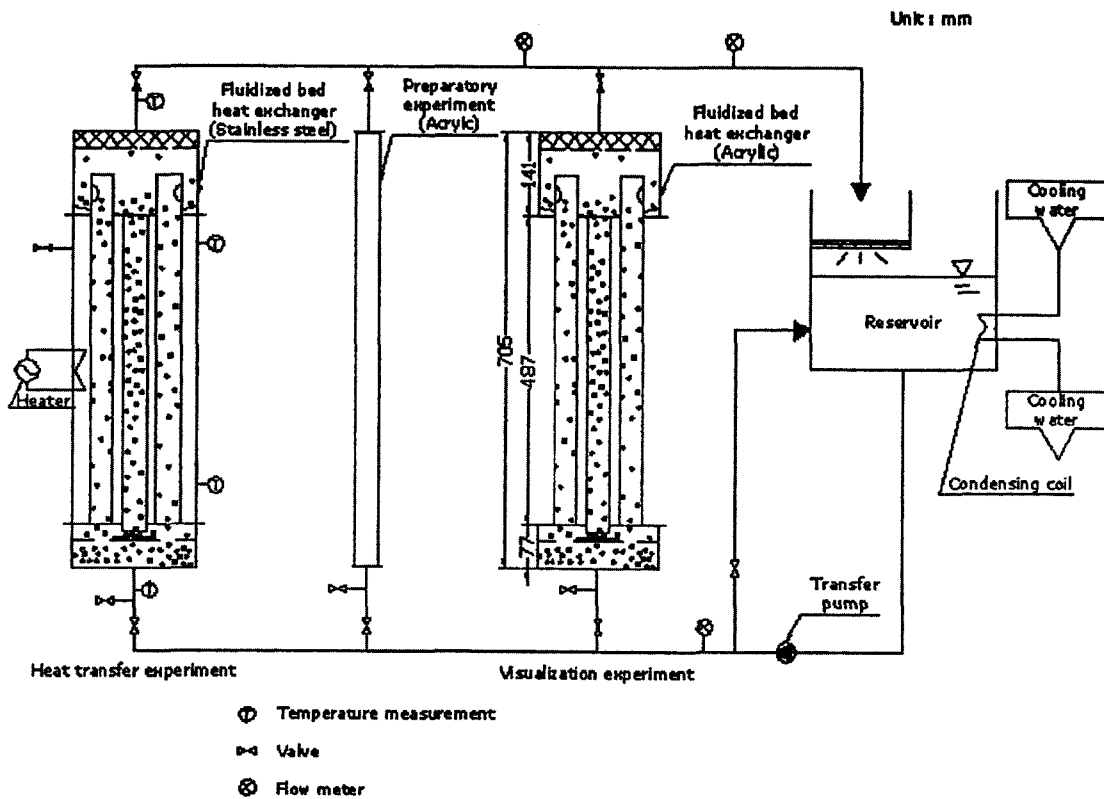


**Fig. 1** Schematics of experimental setup

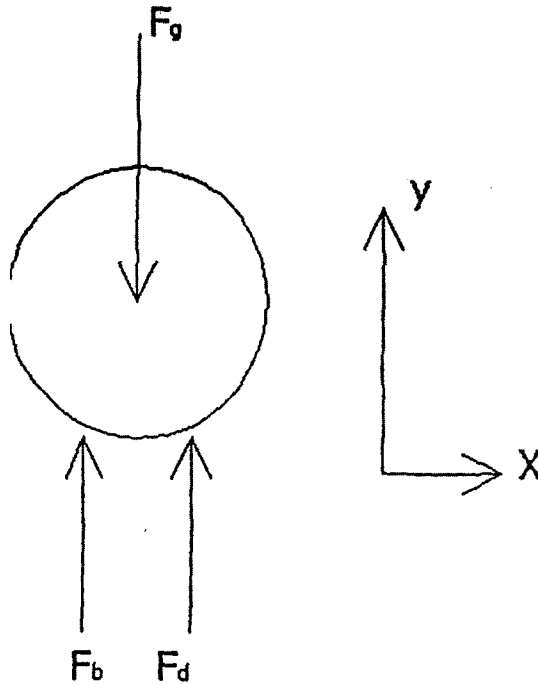


Fig. 2 Force acting on a solid particle

Here,  $U_r$ ,  $C_d$ , and  $A$  represent relative velocity between a particle and stream fluid, frictional drag coefficient, and contact surface, respectively. In this study, two different Reynolds numbers are used. One is  $Re_1$ , which is defined as Eq. (4) and the other is  $Re_2$  defined as Eq. (5). The  $Re_1$  is used for presentation of the drag coefficients, and  $Re_2$  is used for presentation of the heat transfer results.

$$Re_1 = (U_r d_p) / \nu_w \tag{4}$$

and

$$Re_2 = (V dt) / \nu_w \tag{5}$$

where  $\nu_w$  is the kinematic viscosity of fluid. The force balance yields to the following equation ;

$$-F_g + F_b + F_d = 0 \tag{6}$$

Substituting gravity force ( $F_g$ ), buoyancy force ( $F_b$ ), and drag force ( $F_d$ ) into Eq. (6);

$$-m_p g + m_w g + 0.5 \rho_w U_r^2 C_d A = 0 \tag{7}$$

where drag coefficient ( $C_d$ ) is calculated from Eq. (7). The heat transfer coefficient ( $h$ ) is determined from Eq. (8) as follows ;

$$h = \frac{Q}{\pi DL (T_w - T_b)} \tag{8}$$

$$Q = \dot{m}_w c_w (T_o - T_i) \tag{9}$$

where  $\dot{m}_w$ ,  $c_w$ ,  $T_o$ ,  $T_i$ ,  $T_w$  and  $T_b$  are the flow rate of water, specific heat of water, water outlet and inlet bulk temperatures, average wall temperature, and average water temperature, respectively. The heat exchanger for heat transfer measurement was heated with a stainless band heater (5 kW, single phase, AC), and the test section was insulated with an asbestos tape and a glass wool of 4 cm thickness. The stainless band heater was wrapped around the stainless shell, and electric current was supplied to the heater. The shell side of the heat exchanger was filled with water. Thus, the heat was supplied to the shell-side water first, and then to the test tube. The temperatures on each tube wall were measured with k-type thermocouples at three wall positions ; entrance, mid, and exit as shown in Fig. 3. Slits of 10 mm length, 2 mm width, 0.7 mm depth were machined on the outer surface of tube for measuring the wall temperature. Thermocouples were attached in the slit using the thermal epoxy (Omegabond 400, Omega Co.). Teflon coated k-type thermocouples of 0.3 mm diameter were used. In addition, a thermocouple probe was placed at a test duct inlet and exit for measuring bulk fluid temperatures of inlet and outlet water. Over the range of test conditions, the maximum deviations between the wall-to-bulk fluid temperature differences at three positions of test section ; entrance, middle, and exit as shown in Fig. 4 were within 10.5%. The ambient atmospheric temperature of 22 °C to 24 °C was maintained during heat transfer measurement. Temperature measurement was done with YOKOGAWA Data logger. A conservative estimate of the accuracy of the temperature measurement was  $\pm 1$  °C. The uncertainty associated with the length scale used in data reduction was  $\pm 1.5$  mm. It was found that for the minimum flow rate, the worst case, the uncertainties for Reynolds number, drag coefficient, and Nusselt number were  $\pm 7.4\%$  and  $\pm 16.4\%$ ,  $\pm 14\%$ , respectively. The uncertainty estimate procedure was described by

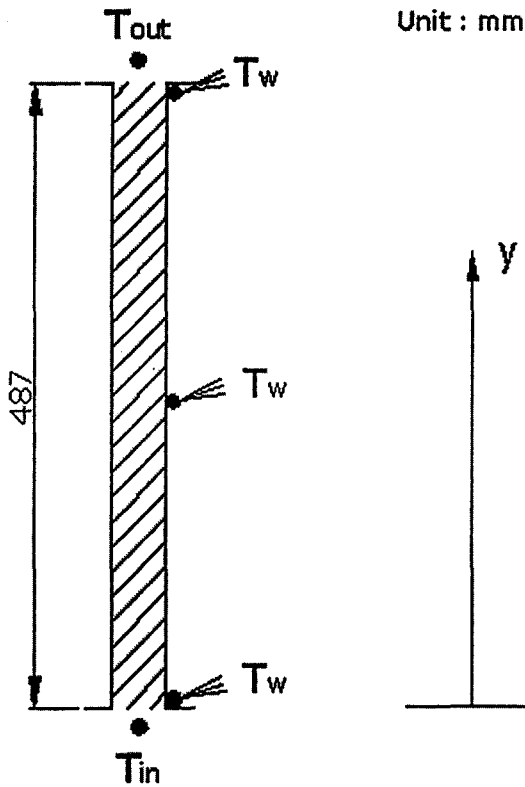


Fig. 3 Heat transfer test tube

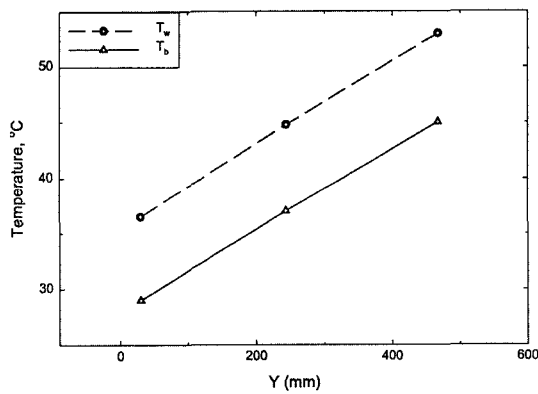


Fig. 4 Variation of  $T_w$  and  $T_b$  along the axial distance

Kline and McClintock (1953).

### 3. Results and Discussion

The fluidized bed heat exchanger can maintain a clean surface because the surface is always hit with solid particles during operation. The

Table 2 Particle flow velocity for collision

Classification	Particle velocity range for collision	
	Minimum	Maximum
Case (A)	0.346 m/s	1.0 m/s
Case (B)	0.278 m/s	0.7 m/s
Case (C)	0.284 m/s	0.8 m/s
Case (D)	0.550 m/s	1.25 m/s
Case (E)	0.627 m/s	1.3 m/s
Case (F)	0.648 m/s	1.3 m/s

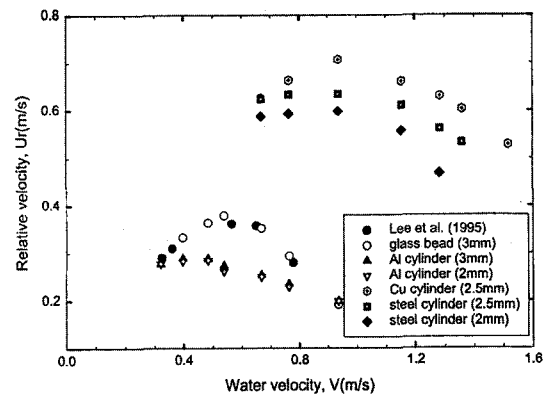


Fig. 5 Relative velocity versus water velocity

hitting velocity range at the wall is shown in Table 2. For higher density materials, collisions started at higher flow velocities because higher densities led to higher solid flow frictional resistances. Different material or geometry should influence the particle behaviour near the wall, and the effects need further research. Water flow velocity was determined from the measured flow volume and the solid particle velocity was measured using the CCD camera. The difference between water and solid particle velocity is defined as a relative velocity. Water temperature was maintained around 23 °C. Figure 5 represents the relative velocities of solid particles in the tubes. The relative velocities for all the particles usually increased, and then decreased with increasing water velocities. This phenomenon was more noticed for the glass beads and coppers. The increase in relative velocity means the decreases in fluid flow frictional resistance. The fluid flow frictional resistance is supposed to be a complex function of density, particle geometry, and surface

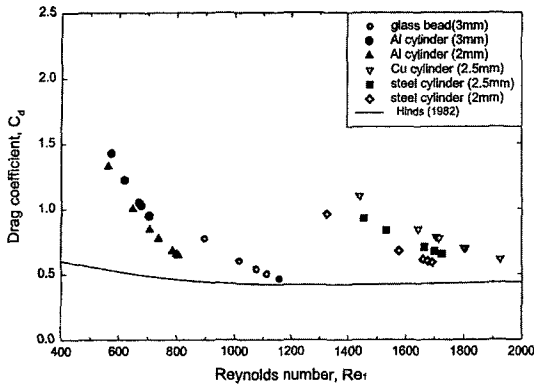


Fig. 6 Drag coefficient versus Reynolds number

area. Figure 5 shows that Lee et al.'s data (1995) agree well with the present work for the glass beads. The variations of drag coefficients against Reynolds number ( $Re_1$ ) based on particle diameter are illustrated in Fig. 6. Drag coefficients ( $C_d$ ) were obtained from Eq. (7). The higher drag coefficients occurred at higher density materials. It was because the solid particles having higher densities have higher viscous resistances. Drag coefficients at all the particles decreased with increasing Reynolds number ( $Re_1$ ). It might be attributed to the fact that drag coefficients were inversely proportional to relative velocities ( $U_r$ ) as shown in Eq. (7). For a comparison, Hinds' data (1982) with the glass beads were included. They were lower than the present results. This might be attributed to the fact that Hinds' work was performed for external flow.

Figure 7 shows the heat transfer coefficients in a fluidized bed heat exchanger with circulating solid particles. The particles flowing with water periodically hit the tube wall, break the thermal boundary layer, and increase the rate of heat transfer. Particularly when the flow velocity is lower, the effect is more pronounced. It is speculated that, as the flow velocity decreases, the hitting frequency may increase, and thus increases the heat transfer. However, over the flow velocity of  $V=1.0$  m/s, the heat transfer coefficients are lower than those without circulating the solid particles (solid line). It is supposed that the solid particles intervene with growing turbulent eddies. The turbulent mixing is closely related to the

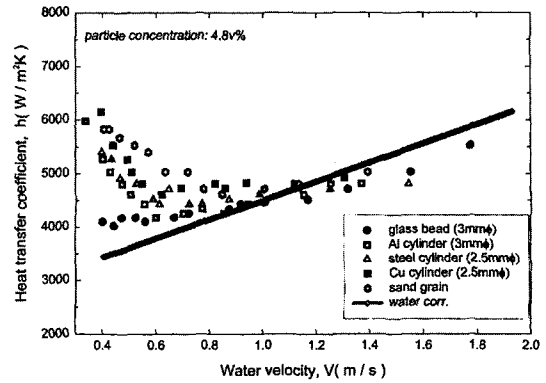


Fig. 7 Improvement of the heat transfer through operation a fluidized bed

increase in heat transfer coefficients at higher water velocities. The heat transfer coefficients with circulating solid particles might be much higher than without circulating solid particles in actual thermal industrial heat exchangers with fouling environmental conditions.

The solid particle volume fraction of 4.8% is maintained at the test section. The sand grains yield the highest heat transfer coefficients. The rough geometries of sand grains may have augmented formation of turbulent mixing. Figure 8 shows the normalized Nusselt numbers—Nusselt numbers with solid particles divided by the Nusselt numbers without solid particles. Below the Reynolds number ( $Re_2$ ) of 5,000, the increase in heat transfer is in the order of sand, copper, steel, aluminum, and glass. This behaviour might be attributed to the parameters such as surface roughness or particle heat capacity. Figure 8 shows that the increase in the normalized heat transfer is higher at lower Reynolds number ( $Re_2$ ) because the hitting frequency of solid particle to the surface is higher.

Main advantage of a liquid fluidized bed heat exchanger is the prevention of fouling. Fouling experiments were conducted at the heat transfer loop. To accelerate fouling, 25,500 ppm of ferric oxide ( $Fe_2O_3$ ) was added to the flowing medium. Ferric oxide was chosen because it was one of the main component of a common fouling deposit. The ferric oxide used in the present study was a mean particle diameter of  $0.98 \mu m$  and a specific

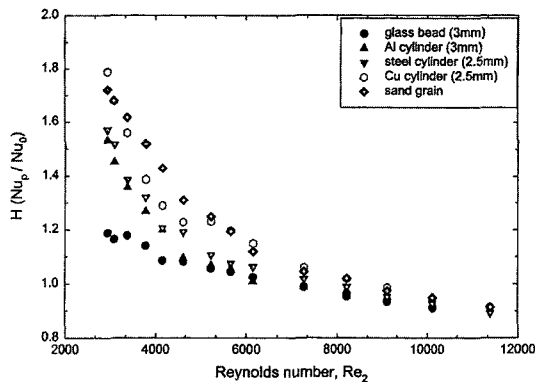


Fig. 8 Normalized Nusselt number

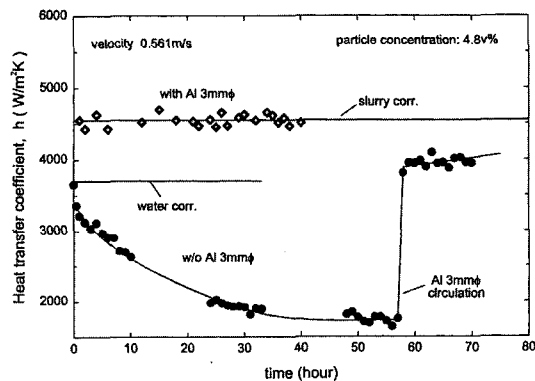


Fig. 9 Cleaning effect of the fluidized bed on  $Fe_2O_3$  scale

gravity of 5.12. The fouling experiment was initiated by pouring an adequate amount of ferric oxide into the circulating water after the system was thermally stabilized. As time elapsed, the ferric oxide deposited at the tube wall yielding heat transfer degradation. The fouling curves were shown in Fig. 9. The flow velocity was maintained at 0.561 m/s. Experiments were conducted in two different ways—one with aluminum particles from the start (shown as open symbol in figure), the other aluminum particles added after sufficient fouling occurred (shown as dark symbol). Figure 9 showed that the heat transfer coefficient maintained the initial value when the aluminum particles were circulated from the start. The solid particles were thought to prevent the ferric oxide buildup continuously hitting the tube wall. When the foulant-water mixture was circulated without aluminum particles, the heat

transfer coefficient rapidly decreased. The fouling curve represented an asymptotic shape, which was typical in particulate fouling. The aluminum particles were added after 58 hours of operation, when the heat transfer decreased to about 40% of initial value. The heat transfer increased immediately, and approached to that of the clean slurry flow.

#### 4. Conclusion

- (1) At flow velocities lower than 1.0 m/s, the particles augmented the heat transfer, and the heat transfer coefficients decreased with increasing flow velocities except the glass bead.
- (2) The heat transfer characteristics are believed to be closely related with the tube wall hitting frequency of the flowing particles.
- (3) Below the Reynolds number of 5,000, the increase in heat transfer according to materials was in the order of sand, copper, steel, aluminum, and glass.
- (4) Fouling tests using ferric oxide revealed that the particles effectively removed the pre-existing deposit as well as the deposit buildup.

#### Acknowledgment

This work was supported by 『Korea Sea Grant Program』 of the Ministry of Maritime Affairs and Fisheries (MOMAF-2000-101-H2090)

#### References

Adomeit, P. and Renz, U., 1994, "The Deposition of Fine Particles from Aqueous Suspensions," *Proc. 10th Int. Heat Transfer Conf.*, Vol. 5, pp. 207~212.

Fraley, L, Lin, Y. Y., Hsiao, K. H. and Solbakken, A., 1983, "Heat Transfer Coefficient in Circulating Bed Reactor," *ASME Paper 83-HT-92*, Seattle.

Grace, J. R., 1986, "Heat Transfer in Circulating Fluidized Beds." In *Circulating Fluidized Bed Technology* (Edited by Basu), pp. 63-81, Pergamon Press, Canada.

Hinds, W. C., 1982, *Aerosol Technology*, Chap.

3, Wiley & Sons, New York.

Kiang K. D., Liu, K. T., Nack, H. and Oxley, J. H., 1976, "Heat Transfer in Fast Fluidized Beds," In *Fluidization Technology* (Edited by Keairns), Vol. 2, pp. 471~483, Hemisphere, Washington, DC.

Kim, N. H. and Lee, Y. P., 1995, "A Study on The Pressure Loss, Heat Transfer Enhancement and Fouling Control in Liquid Fluidized Bed Heat Exchangers," *Proc. of Fouling Mitigation of Industrial Heat Exchange Equipment, An International Conference*, San Luis Obispo, California, pp. 421~433.

Kline, S. J. and McClintock, F. A., 1953, "Describing Uncertainties in Single-Sample Experiment," *Mechanical Engineering*, Vol. 75, pp. 3~8.

Lee, K. B., Jun, Y. D. and Park, S. I., 2000, "Measurement of Heat Transfer Rates and Pressure Drops in a Solid Particle Circulating Fluidized Heat Exchanger," *Korean Journal of Air-Conditioning and Refrigeration Eng.*, Vol. 12, No. 9, pp. 817~824 (in Korean).

Lee, Y. P., Yoon, S. Y., Jurng, J. S. and Kim, N. H., 1995, "Mechanism of Fouling Reduction and Heat Transfer Enhancement in a Circulating Fluidized Bed Heat Transfer," *Korean Journal of Air-Conditioning and Refrigeration Eng.*, Vol. 7, No. 3, pp. 450~460 (in Korean).

Mickley, H. S. and Trilling C. A., 1949, "Heat Transfer Characteristics of Fluidized Beds," *Ind. Engng Chem.* 41, pp. 1135~1147.

Stromberg, L., 1982, "Fast Fluidized Bed Combustion of Coal," *Proc. 7th International Fluidized Bed Combustion Conference*, Vol. 2, pp. 1152~1163.

### Appendix

#### A.1 Calculation of fluid flow velocity in a tube

The vertical shell and tube type fluidized bed heat exchanger with three tubes was used. The fluid flow is assumed to be negligible in the mid tube because solid particles accumulated during operation at least a third of the tube as shown in Fig. A1. From continuity equation, the following

equation is given by :

$$\pi \frac{D^2 U}{4} = 2\pi \frac{d^2 V}{4} \tag{A1}$$

$$V = U \frac{D^2}{d^2} \frac{1}{2} \tag{A2}$$

$$Re_2 = \frac{Vd}{\nu} \tag{A3}$$

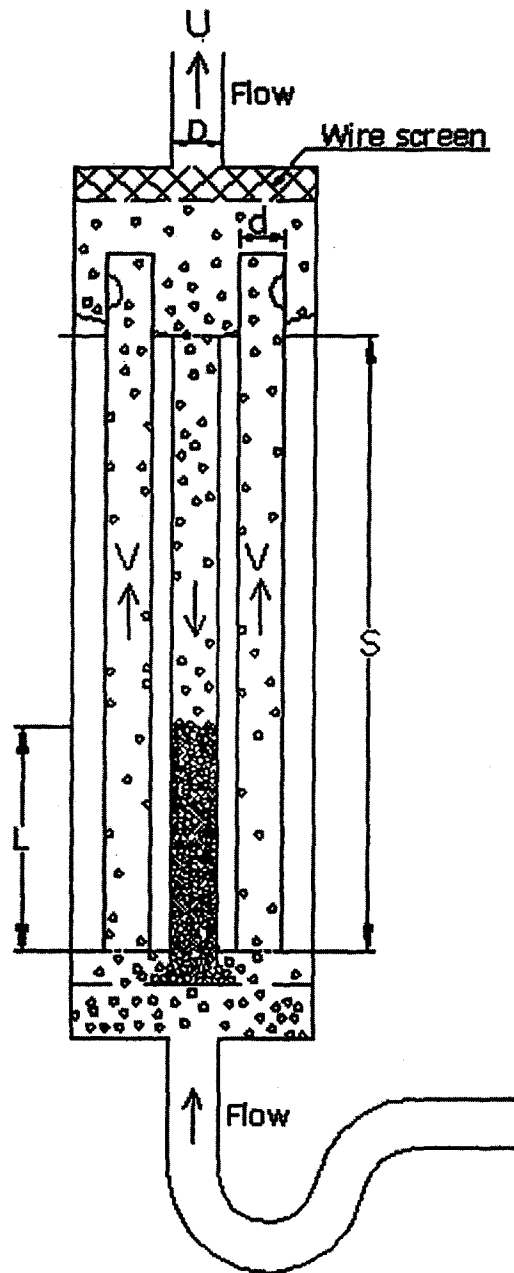


Fig. A1 Principle of particle circulation